

Relative Binding Affinities of Alkali Metal Cations to [1₈]Starand in Methanol: Computational and Experimental Studies

Sungu Hwang, Kwan Hee Lee, Gean Ha Ryu,[†] Yun Hee Jang,[‡] Sang Bok Lee,[§] Woo Young Lee,^{||} Jong-In Hong,* and Doo Soo Chung*

Department of Chemistry, Seoul National University, Seoul 151-742, Korea

Received September 20, 1999

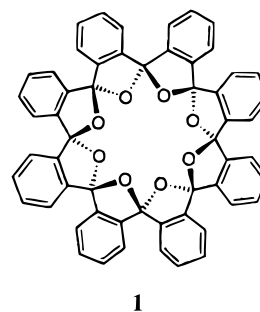
The binding affinity and selectivity of a new ionophore, [1₈]starand (**1**), toward alkali metal cations in methanol were examined through NMR titration experiments and free energy perturbation (FEP) and molecular dynamics simulations. The preference was determined to be K⁺ > Rb⁺ > Cs⁺ > Na⁺ ≫ Li⁺ in both FEP simulations and NMR experiments. The FEP simulation results were able to predict the relative binding free energies with errors less than 0.13 kcal/mol, except for the case between Li⁺ and Na⁺. The cation selectivity was rationalized by analyzing the radial distribution functions of the M–O and M–C distances of free metal cations in methanol and those of metal–ionophore complexes in methanol.

Introduction

[1_{*n*}]Starands, a new class of macrocyclic molecules, were recently synthesized by Lee and co-workers.^{1–4} These highly preorganized molecules are expected to form stable complexes selectively with specific metal cations.^{1,3} In this work, we investigated the binding affinities and selectivities of [1₈]starand (**1**) toward alkali metal cations in methanol. For this purpose, free energy perturbation (FEP) and molecular dynamics (MD) simulations were carried out on the complexes of **1** with Li⁺, Na⁺, K⁺, Rb⁺, and Cs⁺, and the simulation results were checked against NMR titration results.

Binding affinities of alkali metal cations to ionophores are usually measured from water–chloroform extraction experiments.⁵ However, Bayly and Kollman⁶ used pure water as a solvent in their FEP simulation to interpret the salt-extraction experiments, and Åqvist and co-workers⁷ performed their FEP simulation of alkali–metal complexation of an ionophore⁸ in methanol to elucidate the salt-extraction experiments from water to chloroform. The use of polar solvents in the simulations is mainly due to the difficulties in carrying out the simulations in water-saturated chloroform with counteranions.⁶ First,

the amounts of water and counteranions extracted into chloroform are not exactly known yet. Moreover, the water and counteranions are not expected to be distributed homogeneously in the entire chloroform but to be substantially enriched around the cation–ionophore complexes, so we cannot estimate exactly the amounts around the complexes. Second, a much longer simulation time is required for proper sampling of all the relevant configurations of the cations, counteranions, and water molecules in chloroform. Thus, simulations in water-saturated chloroform with counteranions seem to be impractical at present. Instead, we avoided these problems by performing the investigation, both theoretically and experimentally, in a polar solvent, because the cation–counteranion–water aggregate dissociates in a polar solvent. A theoretical study on the alkali metal cation binding of [1₆]starand was recently reported,⁹ in which aqueous solutions were used. However, [1_{*n*}]starands are insoluble in water, so the results are not verifiable by experiment. We chose methanol as the solvent, rather than pure water, because both the alkali metal cation and the ionophore **1** are dissolved in methanol, and thus the simulations in methanol can be checked against experimental results in methanol. In contrast to the water–chloroform extraction, our simulations were able to predict quantitatively the results from the single-phase experiments performed in methanol.



* Doo Soo Chung: (e-mail) dschung@snu.ac.kr. (Phone) +82-2-880-8130. (FAX) +82-2-877-3025. Jong-In Hong: (e-mail) jihong@plaza.snu.ac.kr. (Phone) +82-2-880-6682. (FAX) +82-2-889-1568.

[†] Present address: Natural Science Research Institute, Jeonju University, Jeonju 560-759, Korea.

[‡] Present address: Materials and Process Simulation Center, California Institute of Technology, Mail Code BI 139-74, Pasadena, CA 91125.

[§] Present address: Department of Chemistry, University of Florida, P.O. Box 117200, Gainesville, FL 32611-7200.

^{||} Deceased on Feb. 15, 1997.

(1) Lee, W. Y. *Synlett* **1994**, 765–776.

(2) Lee, W. Y.; Park, C. H.; Kim, S. *J. Am. Chem. Soc.* **1993**, *115*, 1184–1185.

(3) Lee, W. Y.; Park, C. H. *J. Org. Chem.* **1993**, *58*, 7149–7157.

(4) Hwang, S.; Ryu, G. H.; Lee, K. H.; Hong, J.-I.; Chung, D. S. *Bull. Korean Chem. Soc.* **1998**, *19*, 406–408.

(5) Koenig, K. E.; Lein, G. M.; Strucker, P.; Kaneda, T.; Cram, D. J. *J. Am. Chem. Soc.* **1979**, *101*, 3553–3566.

(6) Bayly, C. I.; Kollman, P. A. *J. Am. Chem. Soc.* **1994**, *116*, 697–703.

(7) Åqvist, J.; Alvarez, O.; Eisenman, G. *J. Phys. Chem.* **1992**, *96*, 10019.

(8) Brown, R.; Jones, W. E. *J. Chem. Soc.* **1946**, 781.

(9) Cho, S. J.; Kollman, P. A. *J. Org. Chem.* **1999**, *64*, 5787–5793.

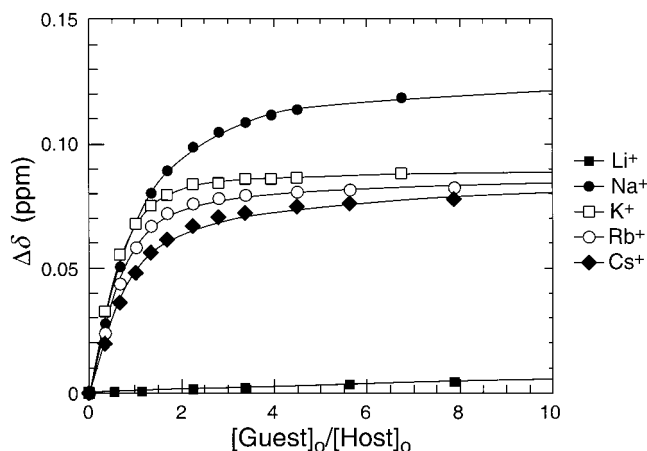


Figure 1. ¹H NMR titrations of 0.89 mM host **1** with 50 mM alkali metal cation (■ Li⁺; ● Na⁺; □ K⁺; ○ Rb⁺; ◆ Cs⁺) at 298 K. Symbols are experimental data points; lines are the best fit curves calculated from nonlinear squares-fitting analysis in CD₃OD. ArH_{ortho} was monitored after each addition of alkali metal. The counteranion is trifluoromethanesulfonate.

Experimental Section

Materials and General Procedure. All solvents were of analytical grade and used without further purification. Starand **1** was prepared as described in the literature,³ and alkali metal trifluoromethanesulfonate salts were prepared from trifluoromethanesulfonic acid (CF₃SO₃H) and alkali metal hydroxides (MOH; M = alkali metal). Alkali metal perchlorate salts were obtained from Aldrich. ¹H NMR spectra were recorded with Bruker DPX 300 (¹H, 300 MHz) and Bruker AMX 500 (¹H, 500 MHz) spectrometers with Me₄Si as an internal standard. Mass spectra were obtained with a Kratos Compact MALDI II, Voyager Biospectrometry Workstation.

Determination of Association Constants (K_a). To assess the relative binding properties of **1**, we performed ¹H NMR titration experiments with alkali metal salts. First, 0.050 M solutions of each alkali metal trifluoromethanesulfonate in CD₃OD were prepared in separate volumetric flasks. Aliquots of each alkali metal cation solution were added to a 0.89 × 10⁻³ M solution of [1₈]starand in CD₃OD. The chemical shifts of the aromatic protons of [1₈]starand were recorded after each addition of the guest solution. The association constants (K_a) were then determined by nonlinear least-squares fitting analyses of the titration curve for simple 1:1 binding, monitoring the chemical shift changes of ArH signals for **1**.^{10,11} The chemical shift changes under fast exchange condition can be written as follows:¹⁰

$$\delta = \delta_1 - \left(\frac{\delta_1 - \delta_c}{2[\mathbf{1}]_0} \right) (B - \sqrt{B^2 - 4[\mathbf{1}]_0[M]_0}) \quad (1)$$

where δ is the observed chemical shift, δ_1 is the chemical shift for free host **1**, δ_c is the chemical shift for the complex, $[\mathbf{1}]_0$ is the initial concentration of **1**, $[M]_0$ is the initial concentration of the metal ion, and

$$B = [\mathbf{1}]_0 + [M]_0 + \frac{1}{K_a} \quad (2)$$

Figure 1 is a typical plot of the observed and calculated titration curves obtained by this method for all alkali metal salts.

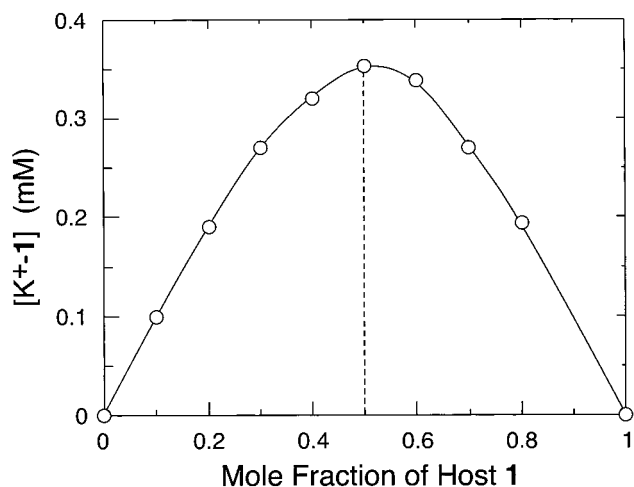
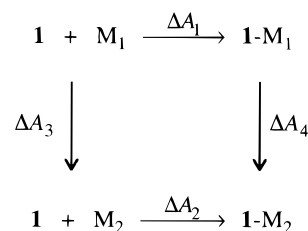


Figure 2. The Job plot for [1₈]starand **1** (1.0 mM) and K⁺ trifluoromethanesulfonate (1.0 mM) in CD₃OD. The concentration of the complex was determined by the procedure described in the ref 12.

Scheme 1. Thermodynamic Cycle for Ions M₁ and M₂ Complexing to the Same Ionophore **1**^a



^a ΔA_1 and ΔA_2 are the free energy changes involved in the binding processes of M₁ and M₂ to **1**. ΔA_3 and ΔA_4 are those involved in the perturbation of M₁ into M₂ in unbound and bound forms, respectively.

Job Plot. Complexation stoichiometry was determined by a Job plot using ¹H NMR spectroscopy.¹² Stock solutions of **1** (1.0 × 10⁻³ M) and potassium trifluoromethanesulfonate (1.0 × 10⁻³ M) in CD₃OD were prepared. Eight NMR spectra were obtained in the following volume ratios (host:guest): 40:360, 80:320, 120:280, 160:240, 200:200, 240:160, 280:120, and 320:80 (μL:μL). The chemical shifts of the aromatic protons of **1** were recorded for each sample, the corresponding concentration of complex was determined for each, and the Job plot was obtained by plotting complex concentration as a function of the mole fraction of alkali metal ions. Figure 2 is the Job plot for **1**–potassium trifluoromethanesulfonate complex.

Calculation Method and Details. The FEP simulation^{13–15} gives the relative binding free energy of two different ions M₁ and M₂ bound to the same ionophore **1** according to the thermodynamic cycle in Scheme 1. Because the free energy A is a state function, the relative binding free energy ($\Delta\Delta A$) is expressed as $\Delta\Delta A \equiv \Delta A_1 - \Delta A_2 = \Delta A_3 - \Delta A_4$. It is obtained by slowly perturbing M₁ into M₂ in both free and bound forms (ΔA_3 and ΔA_4), rather than by attempting the more difficult task of modeling the binding processes (ΔA_1 and ΔA_2).^{13–16} A perturbation from M₁ to M₂ was done by using a coupling parameter λ (0 ≤ λ ≤ 1) to smoothly convert the energy function $E(\lambda)$ of M₁ (λ = 0) into that of M₂ (λ = 1). The free

(12) Connors, K. A. *Binding Constants: The Measurement of Molecular Complex Stability*; John Wiley and Sons: New York, 1987.

(13) Kollman, P. *Chem. Rev.* **1993**, *93*, 2395–2417.

(14) van Gunsteren, W. F.; Mark, A. E. *Eur. J. Biochem.* **1992**, *204*, 947–961.

(15) van Gunsteren, W. F. *Protein Eng.* **1988**, *2*, 5–13.

(16) Cummins, P. L.; Ramnarayan, K.; Singh, U. C.; Greedy, J. E. *J. Am. Chem. Soc.* **1991**, *113*, 8247–8256.

(10) Macomber, R. S. *J. Chem. Educ.* **1992**, *69*, 375–378.

(11) Tjivikua, T.; Deslongchamps, G.; Rebek, J., Jr. *J. Am. Chem. Soc.* **1990**, *112*, 8408–8414.

Table 1. CVFF Parameters for Nonbonding Interactions of Alkali Metal Cations, Converted from the AMBER Parameters of Kollman⁶ According to the Formula $A = \epsilon(2R^*)^{12}$ and $B = 2\epsilon(2R^*)^6$

	AMBER		CVFF	
	ϵ (kcal/mol)	$R^*(\text{\AA})$	A	B
Li ⁺	1.83×10^{-2}	1.137	349.8941	5.06085
Na ⁺	2.77×10^{-3}	1.868	20481.5198	15.06437
K ⁺	3.28×10^{-4}	2.658	167068.0913	14.80518
Rb ⁺	1.71×10^{-4}	2.956	309928.8651	14.51729
Cs ⁺	8.06×10^{-5}	3.395	774055.9141	15.79733

energy change (ΔA) was calculated using the following finite difference thermodynamic integration algorithm:^{17,18}

$$\Delta A = A(\lambda = 1) - A(\lambda = 0) = -RT \ln \left\langle \exp \left(-\frac{\Delta E}{RT} \right) \right\rangle = -RT \sum_{\lambda=0}^1 \ln \left\langle \exp \left(-\frac{E(\lambda \pm \delta\lambda) - E(\lambda)}{RT} \right) \right\rangle_{\lambda} \quad (3)$$

where R is the gas constant and T is the absolute temperature. The bracket denotes an average over a canonical ensemble generated by MD simulations with an energy function $E(\lambda)$ at each Gaussian-quadrature point λ . The MD simulations were performed with the CVFF force field implemented in the *Discover* package.¹⁸ Parameters for alkali metal cations were imported from the AMBER force field of Kollman^{6,19} (see Table 1).^{20,21} These parameters were originally derived for alkali cations in water⁷ and were shown also to be adequate for alkali cations in methanol.^{7,19} The simulations were carried out at 300 K. Periodic boundary conditions were employed with a minimum image model,¹⁸ and a cutoff of 11 Å was used for nonbonding interactions. Solvent molecules were treated explicitly using a $36.00 \times 35.00 \times 29.89$ Å rectangular box containing 560 methanol molecules. An all-atom representation was used for the methanol molecules. The arrangement of the solvent molecules was randomized and equilibrated by a 30-ps simulation. A bare cation solvated in methanol was prepared by soaking the cation into the solvent box with an overlapping solvent molecule removed. For a cation bound to **1** in methanol, the cation was located at the center of mass of **1**, the structure of which had been energy-minimized from the X-ray crystal structure,^{1,3} and this complex was minimized and then soaked into the solvent box with about 30 overlapping solvent molecules removed. These initial structures were minimized for 100 steps to remove any hot spots, i.e., any partial overlap between solvent and solute, and then preequilibrated during 50 ps with a constraint that causes the solute to be located at the center of the solvent box. Then, FEP simulations were carried out to perturb Li⁺ into Na⁺, Na⁺ into K⁺, K⁺ into Rb⁺, and Rb⁺ into Cs⁺. Twenty Gaussian quadrature points were used to go from the initial ($\lambda = 0$) to the final ($\lambda = 1$) state in each FEP simulation. At each point, an MD simulation was carried out with a time step of 1 fs for 0.5 ps of equilibration followed by 1 ps of data collection, and the results were compared to those obtained with a time step of 1 fs for 1 ps of equilibration and 2 ps of data collection. Each FEP simulation was run in both forward (λ from 0 to 1) and backward (λ from 1 to 0) directions, and its hysteresis error was taken as an estimate of the quality of the simulation.^{14,15,22}

(17) Mezei, M. *J. Chem. Phys.* **1987**, *86*, 7084–7088.

(18) *Discover User Guide, version 95.0*, Biosym Technologies: San Diego, 1995.

(19) Sun, Y.; Kollman, P. A. *J. Am. Chem. Soc.* **1995**, *117*, 3599–3604.

(20) Cummins, P. L.; Gready, J. E. *J. Comput. Chem.* **1994**, *15*, 704–718.

(21) http://www.msi.com/support/discover/force_field/add_nonbond.html, M.S.S.S.

(22) Mitchell, M. J.; McCammon, J. A. *J. Comput. Chem.* **1991**, *12*, 271–275.

Table 2. ¹H NMR Data for [1₈]Starand (1**) and Its Metal Trifluoromethanesulfonate Complex in CD₃OD at 25 °C after Addition of 10 Equiv of the Guest**

compound	ArH ^b (ppm)	ArH ^c (ppm)
[1 ₈]starand (1) ^a	7.54	7.33
1 -Li ⁺	7.55	7.34
1 -Na ⁺	7.66	7.47
1 -K ⁺	7.63	7.44
1 -Rb ⁺	7.62	7.43
1 -Cs ⁺	7.62	7.43

^a [1]₀ = 0.89 mM. ^b H_{meta} (dd, $J = 3.4, 5.6$ Hz). ^c H_{ortho} (dd, $J = 3.4, 5.6$ Hz).

Table 3. Association Constants (log K) and the Corresponding Free Energies ($-\Delta G$) of **1 and Alkali Metal Cations at 25 °C**

	Li ⁺	Na ⁺	K ⁺	Rb ⁺	Cs ⁺
12-C-4 (log K) ^{a,c}	2.73	3.64	3.09	3.03	2.94
$-\Delta G$ (kcal/mol)	3.72	4.96	4.21	4.13	4.01
18-C-6 (log K) ^{a,c}		4.42	>5.5 (6.3 ^d)	5.35	4.37
$-\Delta G$ (kcal/mol)		6.03	>7.5 (8.9 ^d)	7.30	5.96
1 (log K) ^b	1.20	3.44	4.16	3.91	3.59
$-\Delta G$ (kcal/mol)	1.64	4.69	5.67	5.33	4.90

^a Conductometric measurements in methanol. ^b ¹H NMR titrations in CD₃OD. Temp, 298 K; $\Delta G (= -RT \ln K)$ is 2.303 log K at 298 K. ^c Reference 24. ^d Reference 42.

Results and Discussion

Complexation Studies with Alkali Metal Ions. The ¹H NMR spectrum of **1** revealed only aromatic proton resonances at δ 7.42–7.21 in CDCl₃, and the ¹³C NMR spectrum displayed four resonances at δ 141.80, 129.69, 122.64, and 114.77 in CDCl₃.³ The simplicity of the spectra discloses a high degree of symmetry of the cyclic polyketal host **1**. In view of the published X-ray analysis of [1₆]starand,² host **1** is expected to have a structure with cyclic polyketal and phenyl rings of up–down–up conformation that can bind cationic guests. In the qualitative examinations, solutions of **1** in methanol demonstrated remarkable solubility toward alkali metal salts, revealing the complexing property of the ligand systems. The ¹H NMR spectra of the complexes showed considerable chemical shift changes, indicating observable binding affinity compared to those of the free host **1**, as shown in Table 2. We observed only the population-averaged aromatic signals for the complexes, which indicates that the exchange of the metal ion between the bulk solution and the complex is faster than the NMR time scale.

Association Constants (K_a). The association constants of **1** with alkali metal cations were obtained by nonlinear least-squares fitting of the ¹H NMR titration in CD₃OD at 25 °C. As shown in Figure 1 and Table 2, the addition of alkali metal ions to a solution of **1** gave a downfield shift of aromatic protons in all cases for host **1** upon complexation, which indicates the presence of cation– π interactions in the solution. The shift of the aromatic protons decreased in the order Na⁺ > K⁺ > Rb⁺ > Cs⁺ > Li⁺. The largest downfield shift was observed for Na⁺ ($\Delta\delta = +0.14$ ppm for ArH_{ortho} with 10 equiv of the guest). The amount of the downfield shift for ArH_{ortho} followed the charge density order (Na⁺, 0.14 ppm; K⁺, 0.11 ppm; Rb⁺, 0.10 ppm; and Cs⁺, 0.10 ppm). The binding affinities of **1** for alkali metal cations as shown in Figure 1 and Table 3 were as follows: K⁺ > Rb⁺ > Cs⁺ > Na⁺ \gg Li⁺. The association constants did not depend on the magnitude of the chemical shift change

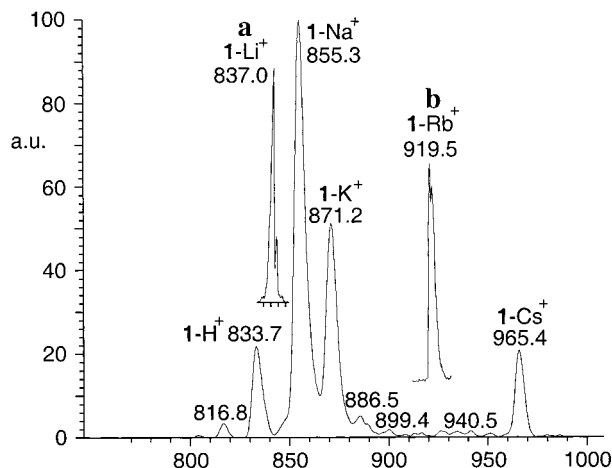


Figure 3. MALDI mass spectrum of a mixture of **1** and alkali metal salts (LiClO₄, NaClO₄, KClO₄, RbClO₄, and CsClO₄) in dihydroxybenzoic acid as matrix in methanol. The peak denoted by **a** was obtained by a Voyager Biospectrometry Workstation using dithranol (1,8,9-anthracenetriol) as matrix in methanol. The peak denoted by **b** did not appear in the mass spectrum of the mixture of alkali metal salts.

induced by metal ions. These observations suggest that the cations interact not only with the four aromatic nuclei of one of the two equivalent binding sites but also with the cyclic ketal oxygens and that the primary interactions between **1** and metal cations would be the cyclic ketal oxygen–metal cation interaction. Host **1** showed higher selectivity for potassium ion than any other alkali metal ion. Stoichiometry between **1** and alkali metal ion can give 1:1, 1:2, or 2:1 binding, because the structure of **1** has two equivalent binding sites. However, the Job plot showed that maximal complexation occurred at 0.5 mole fraction of **1** and the potassium ion, indicating 1:1 binding (Figure 2). This suggests the existence of ionic repulsion between cations when two cations were introduced into the binding cavity of **1** in the case of 1:2 ligand–metal binding and the steric repulsion of **1** in the case of 2:1 ligand–metal binding. Figure 3 shows the mass spectrum from matrix-assisted laser desorption/ionization (MALDI)²³ of a mixture of **1** and alkali ion salts (LiClO₄, NaClO₄, KClO₄, RbClO₄, CsClO₄ in methanol) in dihydroxybenzoic acid as a matrix. Five peaks corresponding to the alkali metal complexes indicate clean formation of 1:1 binding for 1–M⁺ adducts and no fragmentation in the gas phase.

The results of complexation studies for the complexes of **1** and alkali metal cations in CD₃OD at 25 °C are summarized along with those for two other crown ethers in Table 3. Comparison with a cyclic ligand (12-crown-4) having the same number of oxygens for participating in the binding of cations shows that **1** forms stronger complexes with alkali metal cations other than Li⁺ and Na⁺. These results show that a new cyclic ketal **1** having a preorganized structure can act as a better receptor for cation binding than a conformationally mobile and flexible ligand such as 12-crown-4. Host **1** has a pattern of alkali metal cation selectivity similar to that of 18-crown-6.²⁴ The binding affinities of **1** toward alkali metal cations are smaller than those of 18-crown-6, probably as a result

Table 4. Results of FEP Simulations for Alkali Metal Cation Complexes of 1 in Methanol (kcal/mol)^a

	ΔA_3^b	ΔA_4^c	$\Delta \Delta A^d$	$\Delta \Delta G_{\text{exp}}^e$
Li ⁺ → Na ⁺	19.55 ± 0.18	17.86 ± 0.41	−1.69 ± 0.45	−3.05
Na ⁺ → K ⁺	11.51 ± 0.10	10.41 ± 0.16	−1.10 ± 0.19	−0.99
K ⁺ → Rb ⁺	3.87 ± 0.04	4.19 ± 0.04	0.32 ± 0.06	0.34
Rb ⁺ → Cs ⁺	5.04 ± 0.05	5.34 ± 0.06	0.30 ± 0.08	0.43

^a A simulation time of 1 ps for equilibration and 2 ps for data sampling were used at each Gaussian quadrature point. ^b Relative solvation free energies of free cations in methanol. ^c Relative solvation of free energies of cations complexed with **1** in methanol. ^d Relative cation binding affinities of **1** in methanol ($\Delta \Delta A = \Delta A_4 - \Delta A_3$). ^e Calculated from the experimental values determined by NMR studies, Table 3.

of the number of oxygen atoms involved in the cation binding, i.e., four for **1** and six for 18-crown-6.

FEP Simulation in Methanol. The results of the FEP simulations are presented in Table 4. The values obtained with 0.5 ps of equilibration and 1 ps of data collection at each Gaussian quadrature point show almost the same trends as those obtained with 1 ps of equilibration and 2 ps of data collection. Therefore, only the latter results are reported. ΔA_3 and ΔA_4 denote the FEP simulations of the relative free energies of solvation of bare alkali metal cations and alkali metal complexes of **1** in methanol, respectively. These are the average of forward and backward simulations. The hysteresis errors were at most 0.4 kcal/mol in all simulations, and these small errors, along with the convergence of the relative binding affinities upon doubling of the simulation time, indicate that the length of the simulation was adequate to give a meaningful result.^{14,15,22,25} All of the values for ΔA_3 were calculated to be positive, and this indicates that the stability of bare cations in methanol is in the order Cs⁺ < Rb⁺ < K⁺ < Na⁺ < Li⁺, in agreement with experimental results^{26–28} and other calculated results.²⁵ All of the ΔA_4 values were also calculated to be positive, and the stability of the cation complex of **1** in methanol is also in the order of 1–Cs⁺ < 1–Rb⁺ < 1–K⁺ < 1–Na⁺ < 1–Li⁺. The relative binding affinities of **1** for cations in methanol ($\Delta \Delta A$) increases in the order Li⁺ < Na⁺ < Cs⁺ < Rb⁺ < K⁺ (Figure 4), which is in excellent agreement with our experimental results. Note that the FEP simulations gave the relative Helmholtz free energy ($\Delta \Delta A$) since *NVT*(canonical) ensembles were used in this work. However, the calculated results can be compared with the relative Gibbs free energies ($\Delta \Delta G$) from the experiments because the difference between $\Delta \Delta A$ and $\Delta \Delta G$ is negligible in the condensed phase.

The FEP simulations on the alkali metal ion complexes of **1** show a “plateau” selectivity pattern, in which the binding affinity of **1** reaches a maximum at K⁺ and thereafter remains approximately constant as the cation size increases. This behavior is expected for ionophores, which are prevented from interacting effectively with smaller cations by steric or other constraints.²⁹ To explain this selectivity pattern in detail, we investigated the

(25) Thomas, B. E., IV; Kollman, P. A. *J. Am. Chem. Soc.* **1994**, *116*, 3449–3452.

(26) Grootenhuis, P. D. J.; Kollman, P. A. *J. Am. Chem. Soc.* **1989**, *111*, 2152–2158.

(27) Markus, Y. *Ion Solvation*; Wiley & Sons: New York, 1985.

(28) Burgess, M. A. *Metal Ions in Solution*; Ellis Horwood, Ltd.: England, 1978.

(29) Cox, B. G.; Schneider, H. *Coordination and Transport Properties of Macrocyclic Compounds in Solution*; Elsevier Science Publishers B. V.: Amsterdam, 1992; Vol. 76.

(23) Lee, S.; Wyttenbach, T.; von Helden, G.; Bowers, M. T. *J. Am. Chem. Soc.* **1995**, *117*, 10159–10160.

(24) Buschmann, H. J. *J. Solution Chem.* **1987**, *16*, 181–190.

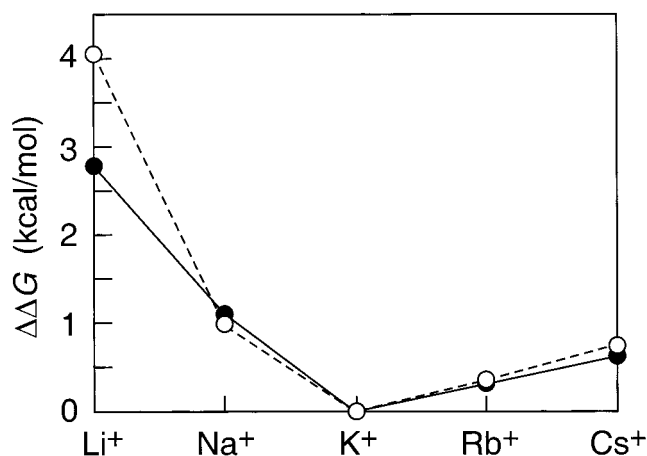


Figure 4. Results of the FEP calculation on the relative affinities of **1** toward the alkali metal cations in methanol. This is a graphical representation of the data given in Table 2. The free energy change ($\Delta\Delta G$; in kcal/mol) during the complexation of **1** with each cation is shown relative to that of **1** with K⁺. The solid line represents the calculated results, and the dashed line represents the experimental results.

structures of the alkali complexes of **1** in methanol obtained from the trajectories of molecular dynamics simulations. Especially, we focused on elucidating why the small cations Li⁺ and Na⁺ are not stabilized in complex with **1** as much as in the free state in methanol.

In general, two principles govern the complexation process: preorganization and complementarity.³⁰ Preorganization^{31,32} is defined as the absence of structural reorganization upon complexation; the more rigidly organized for binding an ionophore is, the more stable will be its complex with ions. In Figure 5, we show the minimum energy structure of each alkali complex of **1** in methanol, along with that of **1** prior to complexation. Here, **1** has a conformation in which eight oxygen atoms adopt an up-down-up arrangement resulting in a spherical cavity.³ The root mean square (rms) deviations between the average structures of **1** before and after complexation were calculated to be only 0.2–0.3 Å for all of the complexes. This shows that **1** has a very rigid and preorganized structure for the alkali cation complexation. Complementarity involves the steric and electrostatic fit between a host and a guest, reflected by a cavity-shape cation-size relationship in the case of ionophores. The radius of the cavity of **1** was estimated to be 1.08 Å by subtracting the van der Waals radius of O (1.40 Å) from the average distance (2.48 Å) from the center of the cavity to the oxygen atoms constituting this cavity. The ionic radii of Li⁺, Na⁺, K⁺, Rb⁺, and Cs⁺ are 0.60, 0.95, 1.33, 1.48, and 1.69 Å, respectively, according to Pauling,^{33–35} and 0.76, 1.02, 1.38, 1.52, and 1.67 Å, respectively, according to Shannon.³⁶ Li⁺ is too small to fully

occupy the cavity, Na⁺ is slightly smaller than the cavity, and the other cations are larger than the cavity. Because the highly preorganized cavity of **1** does not rearrange to wrap around the cations, Li⁺ and Na⁺ cannot fit into the cavity, but K⁺ and other larger cations can fit into the opening of the cavity and can be located at their optimal distances from oxygen atoms. The slight decrease of the binding affinity from K⁺ to Cs⁺ can be attributed to the increase of the ion size. As the ion size increases, the distance between the metal ion and the oxygen atoms of **1** increases, and thus the electrostatic interaction between metal ion and **1** decreases. There are many reports on the alkali cation selectivity of various ionophores with a variety of cavity sizes. For example, 15-crown-5 with a cavity radius of 0.85 Å has a selectivity Na⁺ > K⁺ > Rb⁺ > Cs⁺, and dibenzo-18-crown-6 and 18-crown-6 with cavity radii of 1.2 and 1.3 Å, respectively, have a selectivity K⁺ > Rb⁺ > Cs⁺ > Na⁺ in common for the picrate extraction experiments.³⁷ Host **1** has been determined to have a cavity size comparable to dibenzo-18-crown-6,¹ and its calculated selectivity K⁺ > Rb⁺ > Cs⁺ > Na⁺ ≫ Li⁺ is in accord with other hosts with a similar cavity size.

Because the major interaction is the electrostatic interaction between the cation and the negatively charged oxygen atoms, the M–O distance is very important in the estimation of complementarity. We present in Figure 6 the radial distribution function (RDF) $g(r)$ of the oxygen atoms around the alkali cation in the bare state and in each complex in methanol, along with the coordination number $n(r)$ of the oxygen atoms around the cation as a function of the M–O distance.^{28,38} The position of the first peak of $g(r)$ represents the average distance between the cation and the oxygen atoms constituting the first coordination shell. Because the solvent molecules can reorganize their position rather freely around each cation in the free state, we can take the M–O distance of a bare cation in methanol as the optimum one.¹³ Comparison of this with that of each cation complex of **1** in methanol allowed us to estimate the capability of **1** to stabilize the cation and extract it from methanol.^{30,39} The M–O RDFs of **1**–K⁺, **1**–Rb⁺, and **1**–Cs⁺ complexes have their first peaks at almost the same positions as those of bare K⁺, Rb⁺, and Cs⁺ in methanol. This is because K⁺, Rb⁺, and Cs⁺ can be positioned at the opening of the cavity of **1** at the optimal distance from the surrounding four oxygen atoms. On the other hand, the first peak of the M–O RDF of **1**–Li⁺ in methanol is positioned at 2.2 Å with a large shoulder at 2.5 Å. These are shifted outward from that of bare Li⁺ in methanol positioned at 2.0 Å. The coordination number is about two up to the end point of the first peak and about four up to the end point of the shoulder peak. This suggests that Li⁺ in **1**–Li⁺ is coordinated at an off-center position to two oxygen atoms at a short distance of 2.2 Å and to the other two oxygen atoms at a longer distance of 2.5 Å. In the **1**–Li⁺ complex, the oxygen cavity of **1** cannot be freely rearranged to wrap around the smallest Li⁺ with an optimal Li⁺–O distance of 2.0 Å. Instead, as shown in Figure 5, the cavity is distorted to a form in which Li⁺ can be coordinated to the two oxygen atoms at an off-center position near the periphery of the cavity with an Li⁺–O

(30) Miyamoto, S.; Kollman, P. A. *J. Am. Chem. Soc.* **1992**, *114*, 3668–3674.

(31) Cram, D. J. *Science* **1988**, *240*, 760–767.

(32) Dietrich, B.; Viout, P.; Lehn, J.-M. *Macrocyclic Chemistry: Aspects of Organic and Inorganic Supramolecular Chemistry*; VCH: Weinheim, 1993.

(33) Eisenman, G.; Alvarez, O.; Aqvist, J. *J. Inclusion Phenom. Mol. Recognit. Chem.* **1992**, *12*, 23–53.

(34) Aqvist, J. *J. Phys. Chem.* **1990**, *94*, 8021–8024.

(35) Pauling, L. *The Nature of the Chemical Bond and the Structure of Molecules and Crystals: An Introduction to Modern Structural Chemistry*, 3rd ed.; Cornell University Press: Ithaca, NY, 1960.

(36) Shannon, R. D. *Acta Crystallogr.* **1976**, *A32*, 751.

(37) Ouchi, M.; Hakushi, T. *Coord. Chem. Rev.* **1996**, *148*, 171–181.

(38) Harris, D.; Loew, G. *J. Comput. Chem.* **1996**, *17*, 273–288.

(39) Glendening, E. D.; Feller, D. *J. Am. Chem. Soc.* **1996**, *118*, 6052–6059.

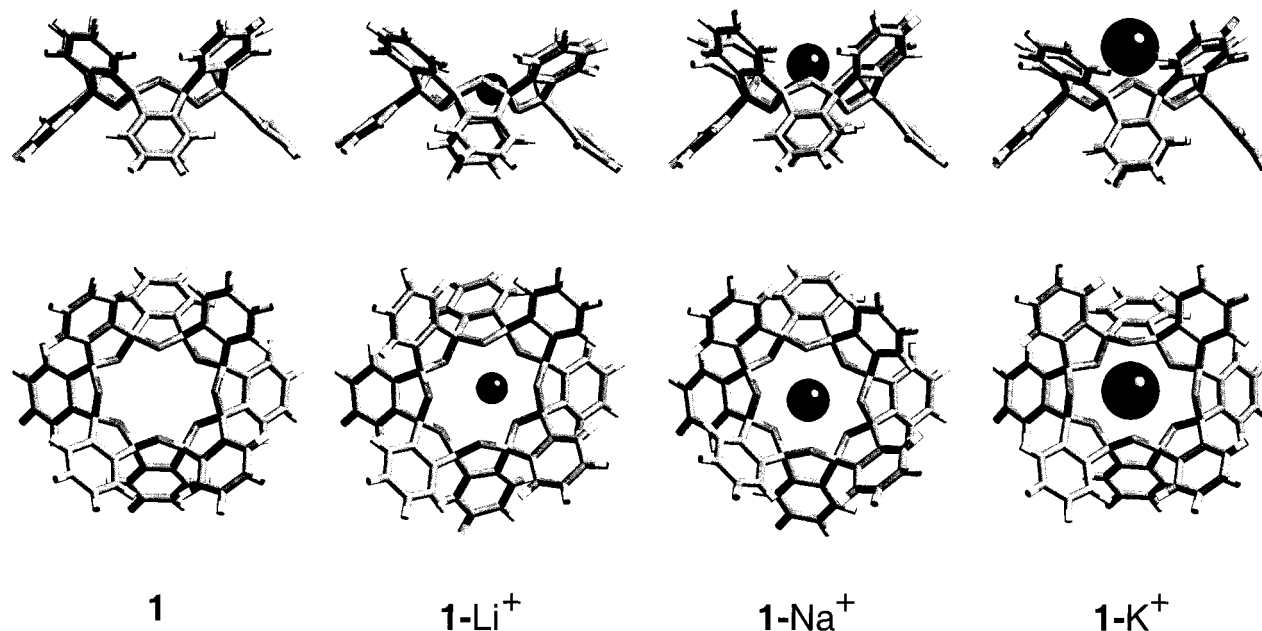


Figure 5. The minimum energy structures of the alkali complexes of **1** in methanol obtained from the molecular mechanics calculations, along with those of **1** in methanol prior to complexation, which were also obtained from the molecular mechanics calculations. Side view (upper) and top view (lower). The metal ions are represented as ball models with Shannon radii.

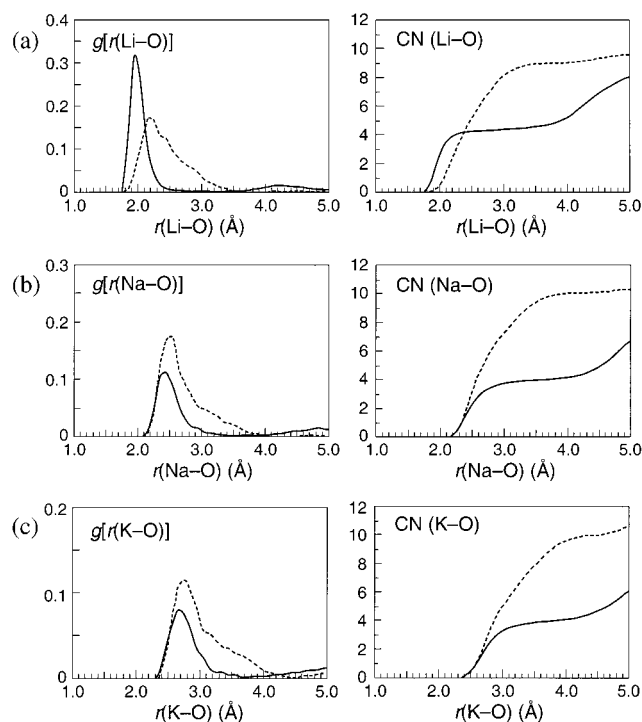


Figure 6. The radial distribution functions (left) and the coordination number (right) of the oxygen atoms around the cation M^+ in free M^+ and $1-M^+$ complex in methanol. (a) Li^+ , (b) Na^+ , and (c) K^+ . The solid line represents the free M^+ in methanol, and the dashed line represents $1-M^+$ complex in methanol.

distance of 2.2 Å. As a result, Li^+ is not stabilized as much as in its bare state in methanol.

We can also see from Figure 5 that the smallest Li^+ is sunk below the opening of the upper cavity of **1**, whereas other cations are displaced out of the cavity. The number of solvent molecules coordinating with Li^+ through their oxygen atoms is only one, and the attractive Coulombic interaction exerted by the solvent oxygen atoms is not

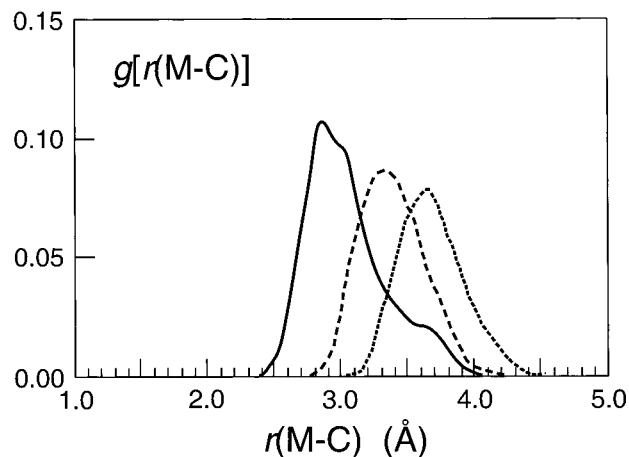


Figure 7. The radial distribution functions between the alkali cation M^+ and the benzyl carbon atoms of **1** in $1-M^+$ complexes in methanol. The solid, dashed, and dotted lines represent the Li^+ , Na^+ , and K^+ complexes, respectively.

as much as in other $1-M^+$ complexes. Li^+ is located in almost the same plane as the carbon atoms, which are directly connected to the oxygen atoms of the cavity. The average distance between Li^+ and these carbon atoms is rather short (around 2.85 Å) compared to that of other alkali complexes (3.35 Å for $1-Na^+$ and 3.65 Å for $1-K^+$) as shown in Figure 7. These carbon atoms carry the positive atomic charge of +0.3e, and they are expected to exert rather large Coulombic repulsions on the Li^+ .⁴⁰ Moreover, the distortion of **1** from the average conformation of 4-fold symmetry in free state in methanol to that of 2-fold symmetry in $1-Li^+$ induces a strain in the $1-Li^+$.

In the case of Na^+ , the shift of the Na^+-O RDF peak was smaller than that of the Li^+-O peak, so we could not judge the relative stability from the $M-O$ RDF

(40) Cho, S. J.; Hwang, H. S.; Park, J. M.; Oh, K. S.; Kim, K. S. *J. Am. Chem. Soc.* **1996**, *118*, 485–486.

analysis alone. However, the $\text{Na}^+\text{-C}$ RDF peak was located at the middle of peaks for $\text{Li}^+\text{-C}$ and $\text{K}^+\text{-C}$, and this reflected the relative instability of the Na^+ complex.

In summary, we have discussed the alkali metal cation selectivity of **1** by analyzing the RDFs of M–O and M–C distances for the metal ions in methanol and those complexed with the host **1**. The relative instability of complexed small cations (Li^+ and Na^+) compared to the same cations in methanol is rationalized by the shift of the M–O RDF peaks corresponding to the first hydration shell and the relative position of the M–C RDF peaks. This explanation is consistent with the widely accepted balance between solvation energies and intrinsic complex stabilities.^{13,41}

Concluding Remarks

The alkali metal cation selectivity of a new ionophore **1** in methanol was examined both theoretically and

(41) Chu, I.-H.; Zhang, H.; Dearden, D. V. *J. Am. Chem. Soc.* **1993**, *115*, 5736–5744.

experimentally. The host **1** forms stronger complexes with alkali metal cations other than Li^+ and Na^+ when compared with 12-crown-4 having the same number of oxygen atoms involved in the metal binding. The FEP simulation gave excellent agreement with the experimental data. The cation selectivity of **1** was in the order of $\text{K}^+ > \text{Rb}^+ > \text{Cs}^+ > \text{Na}^+ \gg \text{Li}^+$, and this was rationalized by analyzing the radial distribution function of M–O and M–C distances in methanol and in the complex with the ionophore.

Acknowledgment. This work was supported by the Korea Science and Engineering Foundation (KOSEF 96-0501-08-01-3), and the Basic Science Research Institute Program (BSRI-97-3416, 3418). S.H. acknowledges a postdoctoral research fellowship from the Korea Research Foundation.

JO991480J

(42) Talma, A. G.; Jouin, P.; De Vries, J. G.; Troostwijk, C. B.; Buning, G. H. W.; Waning, J. K.; Visscher, J.; Kellogg, R. M. *J. Am. Chem. Soc.* **1985**, *107*, 3981–3997.